JOURNAL OF PROPULSION AND POWER
Vol. 13, No. 6, November–December 1997

Open-Loop Performance of a Fast-Response, Actively Controlled Fuel Injector Actuator

Yedidia Neumeier,* Aharon Nabi,† Amos Arbel,‡ Moti Vertzberger,‡ and Ben T. Zinn§
Georgia Institute of Technology, Atlanta, Georgia 30332

This paper describes a study of the frequency dependence of a secondary combustion process response (SCPR) produced by a gaseous fuel injector actuator that was developed for the control of unstable combustor oscillations. Initially, two different approaches are presented for determining the SCPR; one uses pressure data measured in a short combustor and the other uses direct measurements of the global combustion zone radiation in a long combustor. The results of both approaches are in good agreement and show that the fuel injector actuator produces a significant SCPR over a 0–800 Hz frequency range. The results also show that the phase lag of the SCPR increases almost linearly with the frequency, suggesting that a pure time delay plays a role in the mechanisms that control the SCPR. Additional studies presented in the paper investigate the dependence of the SCPR on the characteristics of the fuel actuator and the main injector geometry. These show that the SCPR strongly depends on the location of the modulated fuel stream injection relative to the location of the primary combustion process, and that a larger SCPR is obtained when the secondary, modulated, fuel stream is injected directly into the primary combustion zone.

Nomenclature

C = speed of sound, m/s
C_p, C_v = specific heats at constant pressure and volume, J/(kg K)
e = specific internal energy, J/kg
h = specific enthalpy, J/kg
K_N = nozzle flow rate constant, $m^2\sqrt{K}/(ms)$, Eq. (3)
$\dot{m}$ = mass flow rate, kg/s
p = pressure, n/m^2
$\dot{q}$ = rate of heat addition or removal, W
R = gas constant, J/(kg K)
T = temperature, K
V = volume, m^3
γ = specific heat ratio
ρ = density, kg/m^3
τ = time constant, s, Eq. (7)

Introduction

COMBUSTION instabilities in propulsion systems and rocket motors occur when the combustion process excites one or more natural acoustic modes of the system.[1] Such instabilities are generally driven by a feedback-type interaction between the flow and combustion process oscillations; energy supplied by an oscillatory combustion process excites one or more natural acoustic modes of the combustor whose oscillations are responsible for the periodicity of the combustion process. Because combustion instabilities may result in failure of the combustor and/or mission, considerable resources aimed at preventing the occurrence of such instabilities have been expended over the years. Until recently, these efforts primarily investigated passive control approaches. These included modifications of the combustion process by, for example, changing the injection system to reduce the magnitude and/or change the frequency dependence of the combustion driving, increasing the combustor's damping by the addition of acoustic liners, preventing the excitation of unstable combustor modes by the addition of injector face baffles, and changing the acoustic properties of the combustor to shift its acoustic modes frequencies away from frequencies where significant combustion process driving occurs. Unfortunately, the development of passive control approaches was generally costly and time consuming, and they often failed to adequately damp the instability. Furthermore, a given passive solution is generally only applicable to a specific system over a limited range of operating conditions and may fail or make things worse when applied to a different combustor. The failure of passive control systems to provide satisfactory solutions has stimulated interest in developing active control systems (ACS) for controlling unstable combustors. These efforts started with theoretical investigations of the subject in the 1950s,[2–4] and were followed by the demonstration of the feasibility of active control of combustion instabilities in the 1980s.[5–16]

A typical actively controlled combustor consists of the combustion chamber, a sensor that detects the instability, an observer that determines the state of the system, a controller that modifies the observer's output to provide a control signal for the actuator and an actuator that perturbs the system in a controlled manner. Ideally, such an ACS offers flexibility that permits its application in different systems, and it should perform effectively over a wide range of system operating conditions. In addition, the ACS should be capable of controlling the performance of systems whose behavior is not fully understood. Finally, it must be significantly less expensive and more dependable than existing approaches for suppressing combustion instabilities. While the development of such ACS was not possible in the past because of the unavailability of needed components and computer capabilities, recent developments of novel materials, microelectronics, and powerful microprocessors have provided the components and computing power needed for the development of effective ACS for unstable combustors.

Presented as Paper 96-2757 at the AIAA/ASME/SAE/ASEE 32nd Joint Propulsion Conference, Lake Buena Vista, FL, July 1–3, 1996; received Aug. 22, 1996; revision received April 28, 1997; accepted for publication June 20, 1997.

*Senior Research Engineer and Adjunct Professor, School of Aerospace Engineering.

†Visiting Scholar, School of Aerospace Engineering; currently Research Engineer, Department of Aeronautical Engineering, Technion–Israel Institute of Technology, Haifa, Israel.

‡Visiting Scholar, School of Aerospace Engineering; currently Research Engineer, RAFAEL, Ministry of Defense, Haifa 32000, Israel.

§David S. Lewis Jr. Chair and Regent's Professor, School of Aerospace Engineering.

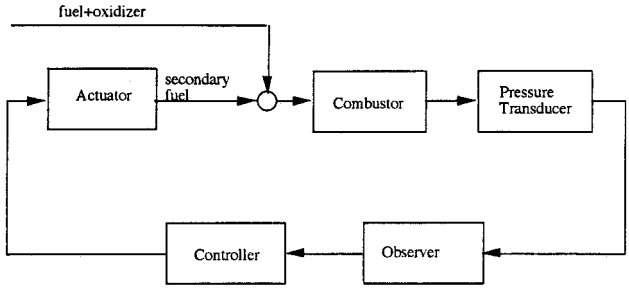

Fig. 1 Schematic of the developed ACS.

The ACS investigated under this program (Fig. 1) damps combustor oscillations by modulating the injection rate of a secondary fuel stream into the combustor, generating a secondary, periodic, combustion process whose objective is to attenuate the unstable combustor oscillations or prevent their occurrence. According to Rayleigh's criterion,[17] the performance of the ACS is optimized when the oscillatory energy that it adds to the system is 180 deg out of phase with the local pressure oscillations.

The developed ACS is based upon an observer that can rapidly identify the frequencies, amplitudes, and phases of the excited combustor modes, which are generally not known in advance, and a fast fuel actuator that modulates a secondary fuel stream to produce combustion process heat release oscillations within the combustor. The feasibility and performance of this ACS were initially investigated using numerical simulations,[18] and subsequently demonstrated on an unstable gas rocket setup.[19]

Effective application of the investigated ACS in the closed-loop control of combustion instabilities requires knowledge of the gain and phase shift that the controller must add to each unstable combustor mode to generate combustion process heat release oscillations out of phase with the unstable mode pressure oscillations. Because each unstable mode oscillates at a different frequency and these frequencies may span a wide range, the frequency dependence of the phase shift and gain that the controller must add to the unstable modes must be known over a wide frequency range. Unfortunately, the characteristics of the secondary combustion process cannot be accurately modeled to predict the frequency dependence of its phase shift and gain because of their nonlinear dependence upon complex fluid mechanical and combustion processes. Therefore, these quantities must be experimentally determined in open-loop tests. The objective of the open-loop tests is to measure the phase delay between the combustion process heat release and actuator control signal oscillations and the ratio of the amplitudes of the combustion process heat release and control signal oscillations, which is referred to as the gain. Together, the measured phase shift and gain describe the secondary combustion process response (SCPR). The remainder of this paper describes the manner in which the open-loop tests were conducted, their results, and the dependence of SCPR upon the actuator and injection system characteristics.

Experimental Facilities

A schematic of the gas rocket motor setup that was used to test the developed ACS is shown in Fig. 2. It consists of a primary reactants (air and methane) feed system, a secondary fuel (methane) injector actuator, a combustor section, a nozzle, a control panel, and a computer-based controller of the secondary fuel actuator. The setup also includes transducers and a photomultiplier that measure the combustor pressure and reaction rate, respectively, and a LabView® system capable of high rate, sample and hold data acquisition.

A proximity sensor, made by Turck, Inc., was used to measure the actuator's motion. It was found that this sensor provided a very high resolution [comparable to that of a linear variable differential transformer (LVDT)] without being affected by the strong magnetic field fluctuations that were generated by the actuator. However, the proximity sensor response to changes in the actuator's movement was not instantaneous because of an electronic filter embedded in its signal conditioner. This delay was experimentally determined, in the relevant frequency range (0–1000 Hz), by comparing the response of the proximity sensor and an accelerometer to white noise excitation, and was subsequently accounted for in the data reduction procedure.

A primary stream of reactants, consisting of premixed air and methane at ambient temperature, was introduced into the combustor through orifices (or a circumferential slot) on the injector plate located on the upstream end of the combustor. The air and methane were separately introduced into a mixing port through calibrated, choked, orifices that provided means for measuring and controlling the flow rate of each reactant by setting the pressure upstream of each orifice to a desired value. The flow through the injector plate was choked to prevent feedback between the combustor pressure fluctuations and reactants supply lines flows. The reactants were injected at an outward orientation relative to the combustor axis, thus stabilizing the primary combustion zone near the combustor walls. Under typical operating conditions, the combustor pressure, premixed reactants line pressure, and fuel and air supply line pressures were 45, 90, and 200 psi, respectively. The combustor pressure was always sufficient for choking the exhaust nozzle. The supply pressure to the secondary fuel injector was 450 psi. Under this operating condition, the flow rates of the primary reactants and secondary fuel were 10 and 0.1 g/s, respectively, resulting in a total combustor power output of 55 kW.

The combustor was made of segments with an i.d. of 1.44 in. and its length could be changed by adding or removing sections of pipes with a large length to diameter ratio to prevent the excitation of transverse modes. This provided a capability for the investigation of axial mode instabilities having different frequencies; high-frequency instabilities are excited in short combustors and vice versa. At its shortest length, the combustor's fundamental mode frequency was around 1800 Hz, while the fundamental mode frequency of its longest configuration was 200 Hz. During operation, the combustor was immersed in a bath of running water to cool its walls.

As shown in Fig. 2, the axis of the investigated combustor was skewed to allow installation of a window through which the total (integrated) CC radicals' radiation from the combustion zone could be passed to the photomultiplier. The photomultiplier was equipped with an optical filter with measured peak at 5166 Å and 40 Å full band width at 50% transmission, for capturing the 5165 Å peak in the Swan band of the CC emission radiated by the hydrocarbon flame.[20] The measured radicals' radiation was used to determine the dynamic response of the global combustion process heat release, as will be discussed later. A second, side-view window, near the injector, was used to visualize the combustion zone.

The actively controlled secondary fuel injector actuator introduced an oscillatory fuel flow into the combustion zone. High-pressure fuel was supplied to the actuator and forced through an annular orifice between the outer wall of the needle's base and its seat before flowing through the injection cavity and the injection orifices into the combustor (Fig. 2). A magnetostrictive actuator, made by Etrema Inc., was attached to the needle and used to oscillate the needle along its axis in response to changes in an electric control signal. The oscillatory, axial motion of the needle produced periodic changes of the annular cross-sectional area between the needle's base and its seat, resulting in a controlled, modulated, secondary fuel flow rate through the annular orifice. The acoustic impedance and pneumatic resistance of the secondary injector's elements that carried the fuel from the supply line to the combustor were sized to maximize the fuel flow rate oscillations at the injec-

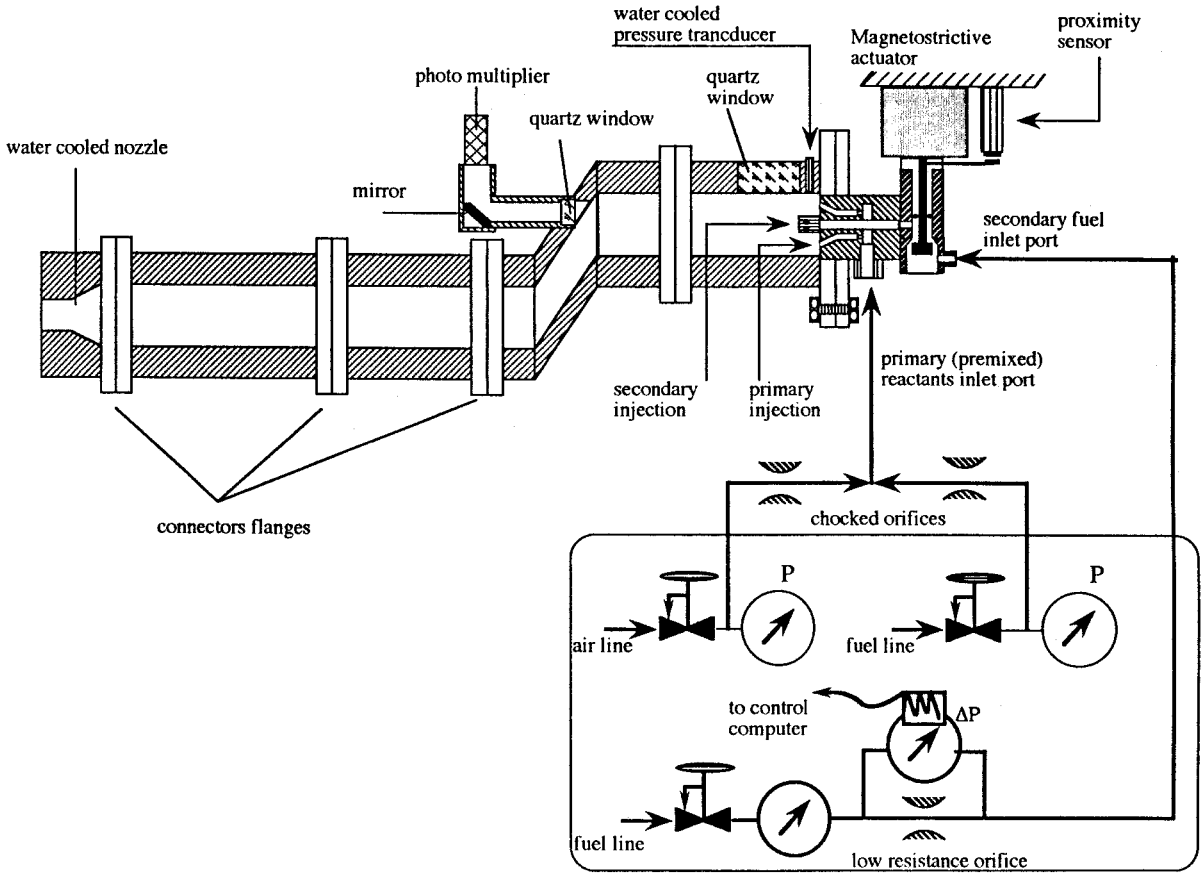

Fig. 2 Schematic of the developed gas rocket setup.

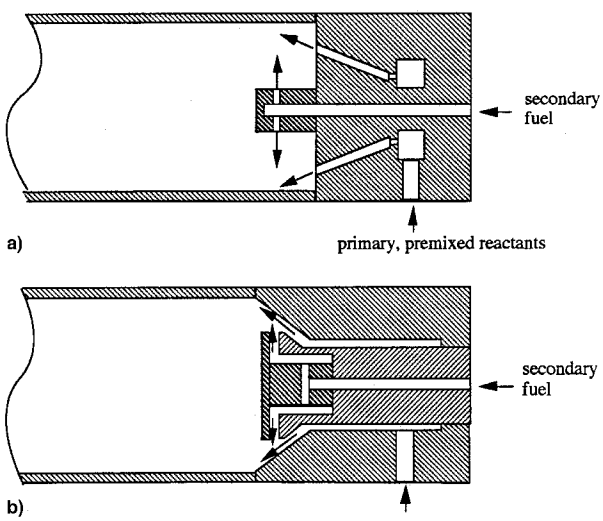

Fig. 3 Schematic of the investigated injectors: a) INJ1 and b) INJ2 configurations.

tor's exit and to minimize the effect of the combustor pressure oscillations upon the injector's performance over a wide frequency range. Injector performance calculations predicted that the injector can produce fuel flow rate oscillations amplitudes of the order of 0.2 g/s over a 0–1,000 Hz frequency range. Such fuel amplitude oscillations can produce 20-kW peak-to-peak heat release rate oscillations if they are fully converted into heat release oscillations.

The electric signal to the actuator consisted of a steady and oscillating component, which controlled the magnitudes of the steady and oscillating flow rates through the fuel injector actuator, respectively. Both signals were generated in the control computer, separately amplified, and then combined into a single control signal that was fed to the actuator.

Two different actuators and injection systems were developed and tested under this program. The actuators were similar in design (Fig. 2) but the annular cross-sectional area of the second actuator was between two to three times larger than that in the first actuator. Each injection system (Fig. 3) supplied the combustor with a primary stream of premixed reactants and a secondary fuel stream that was used to control the instability by generating a secondary, oscillatory, combustion process within the combustor. For further reference, the small and large actuators will be denoted as ACT1 and ACT2, respectively, and the injection systems shown in Fig. 3 will be denoted by INJ1 and INJ2, respectively. The investigated injector/actuator configurations, whose performances are discussed later in this paper, will be described by the notation INJi/ACTi, where the index i = 1, 2 describes the injector and actuator used in the study. It should be pointed out that the ACT2 actuator, which was developed later in the program, could be retrofitted to both injection systems, whereas the ACT1 actuator could be only installed on the INJ1 injector.

Open-Loop Response Studies

This section describes the open-loop studies that investigated the frequency dependence of the phase delay between the combustion process heat release and actuator control signal oscillations and the gain, i.e., the ratio of the amplitudes of the combustion process heat release and control signal oscillations. Together, the measured phase shift and gain describe the SCPR.

A critical issue in the investigation of the SCPR is whether the developed fuel injector actuator can excite combustion process heat release oscillations with amplitudes larger than those generated by the periodic combustion process that drives the instability. If the developed fuel injector actuator could not

excite heat addition oscillations of sufficient magnitude within the combustor, it may not be able to adequately attenuate a fully developed combustion instability. On the other hand, if the amplitude of the heat release oscillations excited by the ACS is larger than the amplitude of the periodic combustion process that drives the instability at its limit cycle, then damping of the instability by the ACS is assured.

Two approaches for determining the SCPR frequency dependence were used in this study. The first used a very short combustor whose fundamental longitudinal acoustic mode frequency was around 1800 Hz, which was significantly above the upper limit of the frequency range of the open-loop studies. Consequently, the operation of this combustor was quiet over the investigated frequency range and the magnitudes of the oscillations driven by the fuel injector actuator were significantly above the combustor noise level. When tests were conducted with the short combustor, high-frequency reaction rate and pressure oscillations driven by an inherent combustor instabilities could be readily observed in the measured pressure and radiation data, and were clearly distinguished from the single frequency oscillations driven by the fuel injector actuator.

The short combustor consisted of a straight pipe with a side-view window next to the injector face. The latter was similar to the one shown in Fig. 2, and was used to measure CC radicals radiation from the combustion region. This window could not view, however, the whole combustion region, and the measured radiation only provided a qualitative description of the characteristics of the secondary combustion process oscillations. Consequently, the characteristics of the SCPR in this combustor were determined from measured dynamic pressure data and a theoretical relationship between the pressure and reaction rate oscillations. The relationship that relates the pressure and heat release oscillations in the short combustor is derived next.

Neglecting kinetic energy terms, the energy equation for a short combustor with uniform properties can be expressed in the following form:

$$\frac{\mathrm{d}}{\mathrm{d}t}\int_V \rho e \, \mathrm{d}V = \dot{q}_{\mathrm{comb}} + \dot{m}_a h_a + \dot{m}_f h_f - \dot{m}_e h_e - \dot{q}_{\mathrm{loss}} \qquad (1)$$

where the terms from left to right are the rate of change of the combustor internal energy, oscillatory heat release, air and fuel enthalpy fluxes into the combustor, enthalpy flux exiting the choked nozzle, and the combustor heat loss, respectively. Assuming a perfect gas behavior and a compact, choked, nozzle, the following relationships can be derived:

$$\frac{\mathrm{d}}{\mathrm{d}t}\int_V \rho e \, \mathrm{d}V = \left(\frac{VC_v}{R}\right)\frac{\mathrm{d}p}{\mathrm{d}t} \qquad (2)$$

$$\dot{m}_e h_e = (K_N p/\sqrt{T_e})C_p T_e \qquad (3)$$

Substituting Eqs. (2) and (3) into Eq. (1), assuming that each dependent variable consists of a steady component and a small amplitude perturbation, e.g., $p = \bar{p} + p'$, neglecting the oscillating component of the heat loss term $\dot{q}_{\mathrm{loss}}$ in Eq. (1), and linearizing the resulting energy equation yields the following linear energy equation:

$$\frac{\dot{q}'_{\mathrm{comb}}}{\bar{\dot{m}}C_p\bar{T}_e} = \frac{p'}{p} + \frac{V\bar{p}}{C_e^2\bar{\dot{m}}}\frac{\mathrm{d}}{\mathrm{d}t}\left(\frac{p'}{\bar{p}}\right) + \frac{1}{2}\frac{T'_e}{\bar{T}_e} \qquad (4)$$

where C_e is the speed of sound at the nozzle entrance. If the convection time of a gas particle from the combustion region to the exit nozzle is much larger than the period of the oscillations, then one may assume that the temperature perturbations generated by the secondary fuel oscillations in the combustion zone are smeared out before reaching the nozzle. In the short configuration of the combustor, the convection time was about 50 ms, which is an order of magnitude larger than the 5 ms period of, say, 200-Hz oscillations. With this simplification, the temperature and pressure oscillations at the nozzle entrance could be related by the following linearized isentropic relationship:

$$\frac{T'_e}{\bar{T}_e} = \frac{\gamma - 1}{\gamma}\left(\frac{p'}{\bar{p}}\right) \qquad (5)$$

Substituting Eq. (5) into Eq. (4) yields the following linear form of the energy equation:

$$\frac{2\gamma}{3\gamma - 1}\frac{\dot{q}'_{\mathrm{comb}}}{\bar{\dot{m}}C_p\bar{T}_e} = \frac{p'}{\bar{p}} + \tau\frac{\mathrm{d}}{\mathrm{d}t}\left(\frac{p'}{\bar{p}}\right) \qquad (6)$$

where

$$\tau = \frac{2\gamma}{3\gamma - 1}\frac{V\bar{p}}{C_e^2\bar{\dot{m}}} \qquad (7)$$

for determining the heat release $\dot{q}'_{\mathrm{comb}}$ oscillations from measured pressure oscillations at high frequencies.

The second approach for determining the SCPR employed the combustor shown in Fig. 2. As discussed earlier, this combustor is equipped with a window on the slanted combustor section that transmits most of the combustion zone radiation to a photomultiplier. In a lean premixed, constant stoichiometry flame that does not produce soot, one can assume that the radicals' radiation intensity is proportional to the heat release rate. However, when the change in the heat release rate is because of a change in the flame's stoichiometry, as in the case when secondary fuel was injected into the premixed reactants flame, such a straightforward relationship between the combustion heat release and the radicals' radiation may not exist. Consequently, before the combustion heat release, oscillations could be related to the measured variations in the measured global radicals' radiation, the increase in the global flame radiation caused by an increase in the secondary fuel injection rate had to be first studied under steady operating conditions. This study revealed that in the lean stoichiometric range of interest, the radicals' radiation from the flame increased nearly linearly with the secondary fuel rate. Using this result and assuming that the combustion efficiency was not affected by the introduction of the secondary fuel injection, it was concluded that the measured change in the radicals' radiation intensity was proportional to the change in the combustion process heat release rate. The steady state correlation was subsequently used to determine the dynamic response of the combustion process to the actuator's modulation of the secondary fuel injection rate.

The combustor shown in Fig. 2 was considerably longer than the short combustor that was used in the first SCPR study. Consequently, several longitudinal acoustic modes of the combustor could be excited within the range of investigated SCPR frequencies, e.g., the fundamental mode frequency of this combustor was 370 Hz. Consequently, the characteristics of the pressure oscillations excited by the fuel injector actuator strongly depended upon the closeness of the secondary fuel modulation frequency to an acoustic mode frequency of the combustor. For example, the secondary heat oscillations could not excite a significant pressure response when operated at an antiresonant frequency of the combustor. Therefore, a model that relates a single acoustic pressure measurement to the characteristics of the heat release oscillations, as was done in the first approach using Eq. (6), could not be used. Also, it is impossible to determine in this combustor the characteristics of the secondary heat release oscillations at or near resonant frequencies. This is so, because at these frequencies the heat release oscillations are strongly affected by inherent instabilities of the combustor as well as by the driving of the secondary

fuel modulations, and it is impossible to separate these two effects to determine the SCPR from the measured radiation data. Consequently, the SCPR was determined in the second approach from direct global flame radiation measurements only at frequencies sufficiently removed from the combustor resonant frequencies where the combustor acoustics did not significantly contribute to the oscillatory reaction rate.

Results and Discussion

In the experiments discussed in the following section, the total flow rate changed between 7–10 g/s, but the stoichiometry remained the same. The total equivalence ratio of the combustor was 0.8 (fuel lean) with 0.6 contributed by the primary premixed reactants, and 0.2 by the mean, secondary fuel. The various analog signals that included the actuator current and displacement, combustion chamber pressure, PMT radiation, and mean secondary flow rate were simultaneously sampled at 5000 Hz by the LabView® data acquisition system. No preconditioning had been applied to the sampled signals.

Figure 4 shows an example of the time dependence and spectra of the pressure and CC radiation signals measured in the combustor shown in Fig. 2, when the secondary fuel injection rate was modulated at 610 Hz. Figure 4b shows that the pressure spectrum is dominated by spikes representing three unstable combustor modes at 370, 740, and 1110 Hz. In general, if a single mode is driven by an unstable combustion process, the amplitudes of its harmonics are smaller than the amplitude of the driven, lowest frequency, mode. The pressure spectrum in Fig. 4b indicates that this was not the case in this experiment as the amplitudes of the higher frequency spikes are larger than the amplitude of the fundamental mode. It should be noted that the pressure transducer was located near the aft end of the combustor where the amplitudes of all axial acoustic modes (which were the only ones excited in this large *L/D* combustor), were maximum. Thus, differences in the measured magnitude of the pressure spikes could not be attributed to the effect of sensor. Consequently, the results shown in Fig. 4b strongly suggest that these modes were independently driven by the combustion process.

An examination of the pressure spectrum in Fig. 4b also shows a small, but clearly distinguishable, spike at 610 Hz, the frequency of the secondary fuel modulation. In contrast, Fig. 4d indicates that only one, large-amplitude, 610-Hz spike is present in the CC radiation spectrum. The dominance of the spike of the driven heat release oscillations in the CC radiation spectrum indicates that under this test condition the fuel injector actuator readily excited heat release oscillations whose amplitude is significantly larger than those that drive the large-amplitude pressure spikes at the resonant frequencies (Fig. 4b).

Figure 4b shows that a fast Fourier transform (FFT) can be used to identify a small-amplitude, periodic, pressure signal near large-amplitude spikes. It was found, however, that an FFT analysis cannot accurately determine the phase of such a small-amplitude signal. Unlike the determination of the amplitude, the determination of the phase is highly sensitive to the frequency at which the FFT integral is evaluated. Because the FFT evaluation is performed at a discrete number of frequencies, it may not be performed at the exact frequency of the secondary combustion oscillations, thus increasing the likelihood of inaccurate phase determination.

To accurately determine the amplitude and phase of the secondary heat release oscillations, the following ensemble-averaging technique was used:

1) The input to the actuator (usually a current) was chosen as a reference signal.

2) Measured data points were correlated with the reference signal by referencing the time of each data point to a specific phase in the period of the reference signal, thus collapsing all of the measured data points into one period.

3) A moving, narrow-width (much smaller compared to the cycle span), window was used to obtain the ensemble average of the time dependence of the collected data over the period of the reference signal. It should be noted that the time dependence of the calculated average is not always sinusoidal.

4) The ensemble-averaged line was curve-fitted with a sinusoidal signal to obtain the corresponding amplitude and phase of the measured data.

Figure 5 presents typical results obtained with this data reduction approach using data measured in the test discussed in Fig. 4. The top to bottom plots on the left side of Fig. 5 show measured data points describing the actuator control signal (current), actuator needle displacement, combustor pressure, and combustion process CC radiation, respectively. The corresponding plots on the right side of Fig. 5 show the ensemble averages of the collected data points (solid lines) and the sinusoidal curves that were fitted to the ensemble-averaged curves (dashed lines).

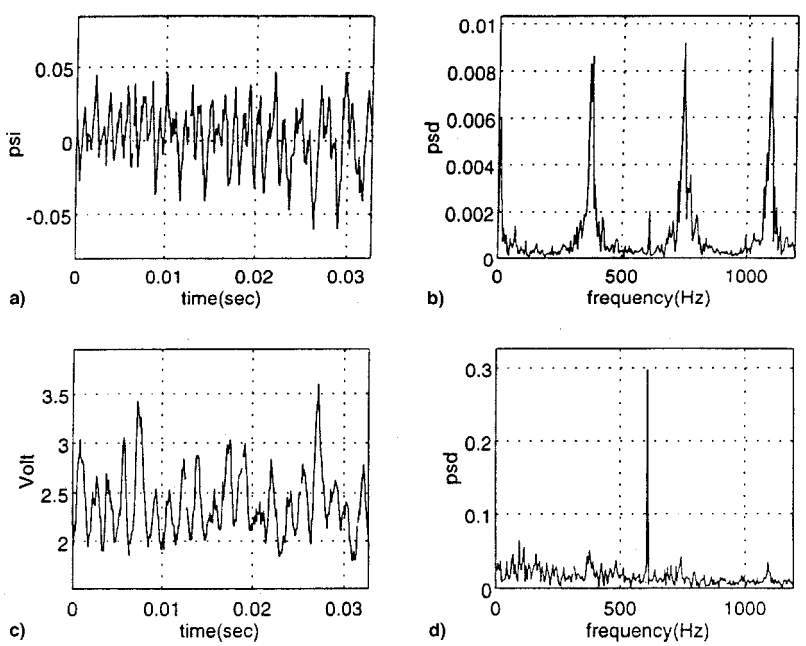

Fig. 4 Time dependence and spectra of the combustor pressure (above) and CC radicals radiation (below) measured in an open-loop experiment in the combustor shown in Fig. 2.

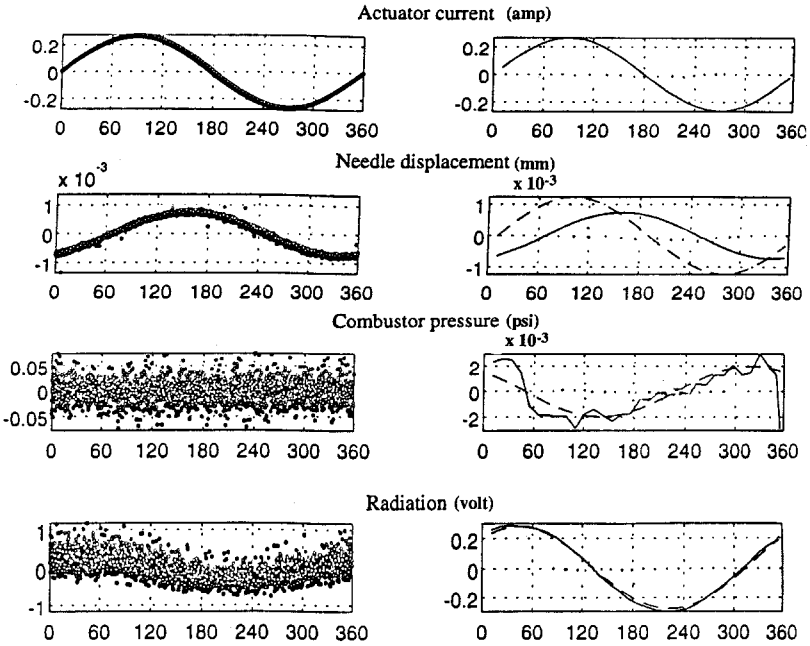

Fig. 5 Measured and ensemble-averaged data describing the actuator current needle, displacement, combustor pressure, and CC radicals radiation obtained in the open-loop experiment whose results are presented in Fig. 4. Dots describe ensemble data, solid lines describe ensemble-averaged quantities, and dashed lines describe the sinusoidal curve fits.

As discussed earlier, unlike the actuator current, pressure, and CC radiation, which were measured by sensors with practically no time delay, the proximity sensor that measured the actuator's needle displacement utilized an electronic filter that introduced a significant phase lag and attenuation to the measured data. This phase lag and attenuation, which were determined in advance by comparing known input signals at various frequencies to the sensor's output, were accounted for in the data reduction procedure by providing the determined sinusoidal signal with a phase lead and a gain relative to the calculated average curve.

Figure 5 shows that both the measured CC radiation and pressure data form clouds of points. However, while the CC radiation cloud exhibits a sine-like shape, such a pattern is not readily apparent in the thick cloud of pressure data points. This difference between the pressure and radiation data is reflected in the presence of high-frequency components in the ensemble average of the pressure data, and the practically sinusoidal shape of the ensemble average of the CC radiation data, which nearly coincides with its sinusoidal curve fit.

The previously described data reduction procedure was applied to the data measured in the open-loop tests to obtain the frequency dependence of the phase and gain of the previously described variables and, in particular, the transfer function between the needle displacement, which closely mimics the fuel injection modulation, and secondary combustion process heat-release oscillations.

The frequency dependence of the gain and phase delay of the secondary combustion process heat release oscillations generated by the fuel injector actuator were independently determined by the previously discussed approaches; that is, the one that used measured pressure and Eqs. (6) and (7), and the one that directly determined the combustion heat release rate from the CC radiation measurements. The results are compared in Fig. 6. The excellent agreement between the two SCPRS that were determined based upon different approaches in two different combustors strongly suggests that the frequency response of the heat addition oscillations generated by the developed fuel injector actuator is practically independent of the acoustic properties of the combustor. Figure 6a shows that the gain decreases with frequency, while Fig. 6b shows that the phase decreases linearly with frequency. The implications of these trends are further discussed later in this paper.

Subsequent studies investigated the dependence of the SCPR upon the injector and actuator characteristics. Figure 7 shows the measured frequency dependence of the phase and gain of the secondary combustion process heat release of two different injector/actuator configurations that consisted of each of the two developed injectors Fig. (3), and the larger fuel injector actuator (i.e., configurations INJ1/ACT2 and INJ2/ACT2). The frequency dependence of the SCPR of the INJ1/ACT2 configuration was determined for various magnitudes of the actuator's needle displacement.

Figure 7a indicates that the phase delay between the heat release and actuator displacement oscillations increases monotonically with the frequency in a nearly linear manner. It should be noted that such linear frequency dependence of the phase is generated by pure time delay. It should be also noted that the short cavity that transfers the fuel from the actuator's orifice to the combustor could only contribute a negligible phase delay because its length was small with respect to the acoustic wavelength in the excited frequencies range. It is most likely that the monotonic increase in the phase between the actuator's motion and the measured radiation oscillations indicates a pure time delay because of the mixing of the secondary fuel with the combustor gas prior to its reaction with the excess oxidizer in the combustion zone.

Figure 7a shows that all of the measured phase data can be closely correlated by a single curve, suggesting that both injectors produce a practical identical time delay between the fuel injection rate and the corresponding secondary combustion process heat release oscillations. This is a surprising result because it was not expected that different injectors would produce an identical time delay.

Figure 7b shows the frequency dependence of the injectors gain; that is, the ratio of the amplitudes of the combustion process heat release and the actuator's needle displacement oscillations. The scatter in the data points in Fig. 7b shows that the gain depends upon the amplitude of the needle's displacement, whose magnitude is indicated next to some of the data points obtained with injector INJ1. Examination of these data shows that the gain is larger for smaller needle displace-

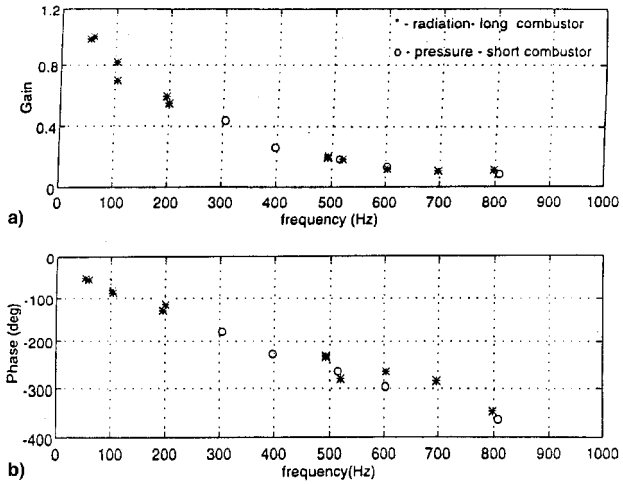

Fig. 6 Comparisons of the frequency dependence of the a) gain amplitude and b) phase of the heat release oscillations produced by the fuel injector actuator obtained from pressure measurements in the short combustor and direct CC radiation measurements in the long combustor.

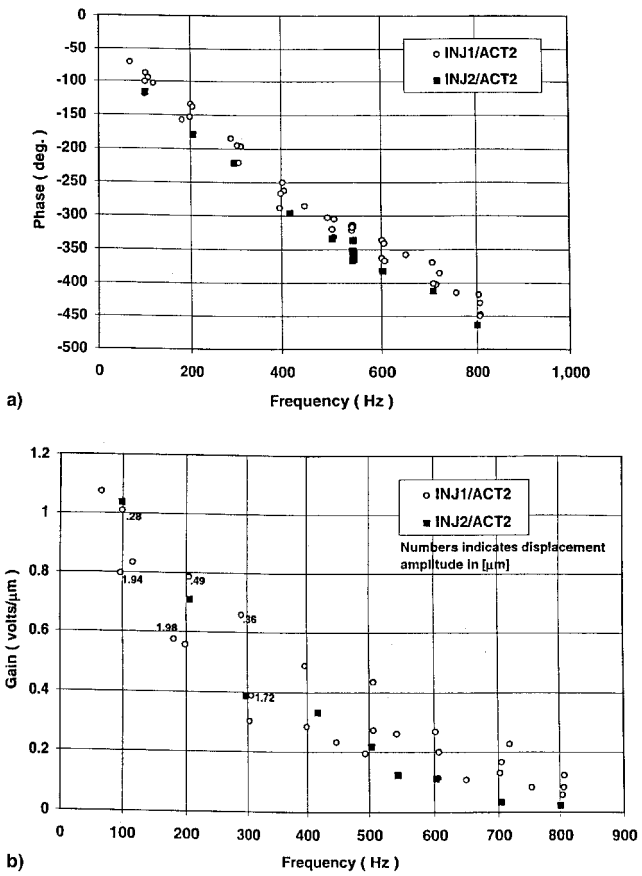

Fig. 7 Frequency dependence of the a) phase difference between heat release and actuator displacement oscillations for two different injector/actuator configurations, and b) the gain of the heat release with respect to actuator displacement oscillations for two different injector/actuator configurations.

ment amplitudes. The reason for this amplitude dependence is explained next.

The developed fuel injector actuator provides the combustor with a fuel flow consisting of a mean and an oscillatory component. The mean flow rate is maintained at a set value by a mean flow rate controller that sends a slowly varying signal to control the mean position of the needle and, thus, the mean area of the actuator's annular orifice and mean fuel flow rate. In addition, the actuator receives a high-frequency signal that sets the needle into high-frequency, back-and-forth, axial oscillations that periodically vary the actuator's orifice cross-sectional area, resulting in a periodic secondary fuel injection rate. As long as the periodic variation of the orifice's area is smaller than its mean area, the periodic change in the orifice's cross-sectional area does not interfere with the mean flow rate through the actuator (Fig. 8a). As the amplitude of the actuator's needle displacement oscillations increases, a threshold amplitude that forces the actuator's orifice to momentarily close at the instant of maximum needle displacement is reached. When the amplitude of the needle's displacement oscillations becomes larger than this threshold value, the orifice remains closed during a portion of the cycle, resulting in an increase in the mean fuel flow rate (Fig. 8b). This forces the actuator's mean flow rate controller to further close the actuator orifice, resulting in additional truncation of the fuel flow rate oscillations Fig. (8c). This discussion indicates that the amplitude of the fuel flow rate modulation cannot exceed the magnitude of the mean fuel flow rate.

During the portions of the cycle when the orifice is closed (Figs. 8b and 8c), the magnetostrictive actuator that is attached to the needle continues its upward motion. The amplitude of this movement is measured by a proximity sensor and used to determine the SCPR gain, which is defined as the ratio of the amplitudes of the heat release and needle displacement oscillations. Thus, as the needle displacement amplitude becomes larger than the threshold value that closes the fuel injector, the magnitude of the gain decreases because its denominator increases while its numerator remains constant at its maximum value. This explains why larger gains are reported in Fig. 7b for lower needle displacement amplitudes.

Figure 9 shows the dependence of the ratio of the amplitude of the combustion process CC radiation oscillations and the mean CC radiation on the needle's displacement amplitude at a frequency of 540 Hz for three different injector/actuator configurations. These results show that the amplitude of the CC radiation oscillations reaches a limiting value at a given needle displacement amplitude and cannot increase beyond this limiting value as the needle displacement is further increased.

To better understand the results of Fig. 9, we should consider the two main processes that control the interaction between the secondary combustion process heat release and needle displacement oscillations. First, consider the variation in the fuel flow modulation amplitude in response to the needle's displacement oscillations. As discussed in the preceding text, the amplitude of the fuel modulation cannot exceed the magnitude of the mean flow rate. Consequently, to increase the amplitude of the fuel flow rate modulation would require increasing the magnitude of the mean flow rate. To illustrate this point, the behavior of the two actuators that were used in this study is qualitatively described in Fig. 10, where the expected dependence of the amplitude of the secondary fuel injection rate modulation upon the amplitude of the actuator's needle displacement is plotted for the large and small actuators operating with two different mean flow rates. Figure 10 indicates that while the ACT2 actuator with the larger orifice provides larger amplitude fuel flow rate modulations for a given amplitude of the needle's displacement oscillations, both actuators can provide the same maximum fuel flow rate oscillations amplitudes if they provide the same fuel mean flow rate.

Another factor affecting the amplitude of the combustion process heat release oscillations is the efficiency of converting the secondary fuel injection rate modulations into combustion process heat release oscillations. Intuitively, one would expect that the ratio of the amplitudes of the combustion process heat release and secondary fuel injection rate oscillations would depend upon the injector design. Examining the configurations of the two investigated injectors (Fig. 3) shows that the INJ1 injector supplies the secondary fuel stream directly into the

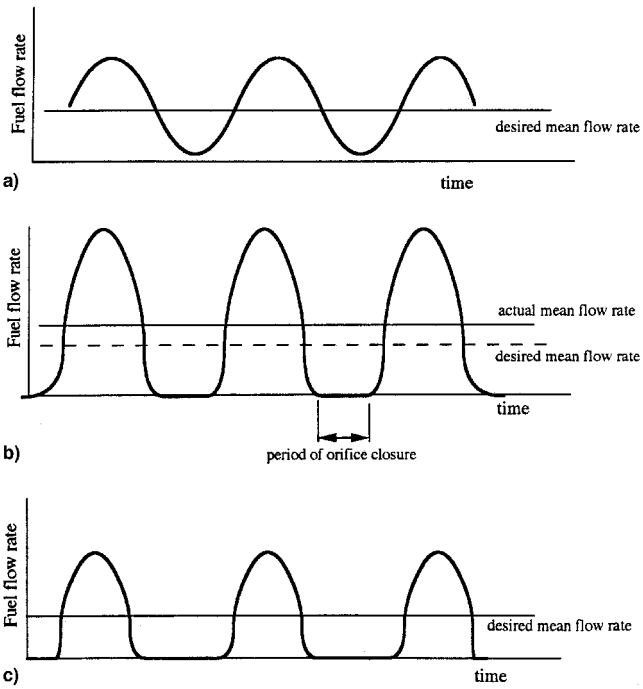

Fig. 8 Qualitative description of the effect of mean flow control upon flow modulation: a) small needle displacement, b) large needle displacement without mean flow control, and c) large needle displacement with mean flow control.

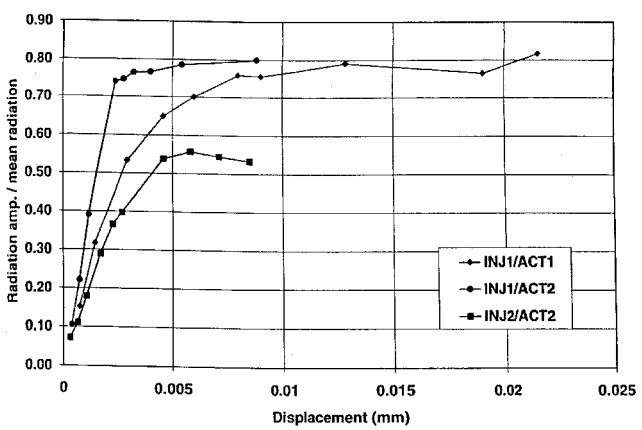

Fig. 9 Dependence of the ratio of magnitudes of the oscillating and mean heat release radiation upon the amplitude of the actuator's needle displacement at a frequency of 540 Hz.

center of the primary combustion zone, whereas the INJ2 injector apparently injects the secondary fuel upstream of the primary combustion region, possibly enabling the secondary fuel to fully or partially mix with the premixed, primary, reactants flow before reaching the combustion zone. This premixing process apparently tends to decrease the magnitude of the attained secondary combustion heat release oscillations. Consequently, the INJ1 injector is expected to provide a more efficient conversion of the fuel injection rate modulation into combustion process heat release oscillations than the INJ2 injector.

On the basis of the previous discussion, one would expect that configurations INJ1/ACT2 and INJ2/ACT1 will produce the largest and smallest secondary combustion process heat release oscillations for a given needle displacement, respectively, while configurations INJ1/ACT1 and INJ2/ACT2 will produce heat release oscillations that fall between these limits. These expectations are supported by the results in Fig. 9, where it is shown that for a given amplitude of the actuator's needle displacement, the amplitude of the secondary heat release oscillations decreased in the following order: INJ1/ACT2, INJ1/ACT1, and INJ2/ACT2.

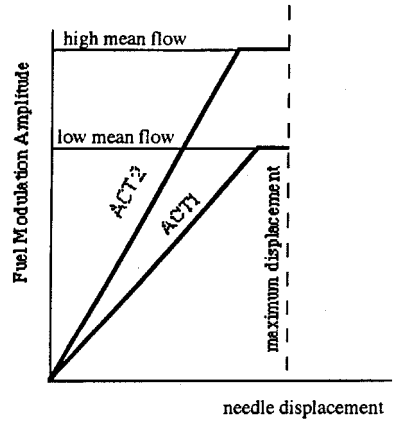

Fig. 10 Qualitative description of the dependence of the fuel modulation amplitude upon the needle displacement for two different actuators and mean flows.

The previous discussion and Figs. 9 and 10 indicate that the smaller ACT1 actuator could provide the same maximum fuel flow rate and heat release oscillations as the larger ACT2 actuator if it could be driven with a larger maximum needle displacement amplitude. This explains why the two configurations INJ1/ACT1 and INJ1/ACT2 that used the same injector, but different actuators, attained the same maximum secondary heat release magnitudes (Fig. 9). It is noteworthy that the maximum amplitude of heat release oscillations that can be excited by the INJ2 injector is significantly smaller than those excited with the INJ1 injector, even when the INJ2 injector used the larger ACT2 actuator.

Summary and Conclusions

This paper presents the results of an investigation of the frequency response of the SCPR produced by a fuel actuator that was developed for active control of combustion instabilities over a 0–800 Hz frequency range. At low frequencies, below the combustor fundamental resonance, the SCPR can be evaluated from pressure data, and at high frequencies it can be determined from direct measurements of the global combustion zone radiation. However, when the SCPR is determined from direct radiation measurements, the experiments must be conducted at frequencies sufficiently removed from the natural acoustic modes of the combustor to assure that the measured SCPR is not affected by acoustic effects.

The measured data indicate that the phase lag of the SCPR monotonically increases with frequency in an almost linear fashion. This suggests that a pure time delay is involved in the mechanism that controls the SCPR. This kind of phase lag behavior poses difficulties in classical linear control approaches.

Additional studies of the dependence of the SCPR upon the characteristics of the injection system and actuator were conducted. Their results show that the SCPR strongly depends upon the location of the modulated fuel stream injection relative to the location of the primary combustion process. Specifically, larger amplitude heat release oscillations were obtained when the secondary, modulated, fuel was injected directly into the primary combustion zone. Also, it was shown that the incorporation of a mean fuel rate controller into the fuel injector actuator limits the amplitude of the fuel modulations developed by the fuel actuator.

Acknowledgments

This research was supported by the Air Force Office of Scientific Research, Contract F49620-93-1-0177. Mitat Birkan was the Technical Moniter.

References

[1]Harrje, D. T., and Reardon, F. (eds.), "Liquid Propellant Rocket Combustion Instability," NASA SP 194, 1972.

[2]Tsien, H. S., "Servo-Stabilization of Combustion in Rocket Motors," *Journal of the American Rocket Society*, Vol. 22, 1952, p. 256.

[3]Marble, F. E., and Cox, D. W., Jr., "Servo-Stabilization of Low-Frequency Oscillations in a Liquid Bipropellant Rocket Motor," *Journal of the American Rocket Society*, Vol. 23, No. 63, 1953, pp. 63–81.

[4]Crocco, L., and Cheng, S. I., *Theory of Combustion Instability in Liquid Propellant Rocket Motors,* AGARDograph No. 8, Butterworths, London, 1956.

[5]McManus, K. R., Poinsot, T., and Candel, S. M., "A Review of Active Control of Combustion Instabilities," *Progress in Energy and Combustion Science*, Vol. 19, 1993, pp. 1–29.

[6]Dines, P. J., "Active Control of Flame Noises," Ph.D. Dissertation, Cambridge Univ., Cambridge, England, UK, 1984.

[7]Bloxsidge, G. J., Dowling, A. P., Hooper, N., and Langhorne, P. J., "Active Control of Reheat Buzz," *AIAA Journal*, Vol. 26, No. 7, 1988, pp. 783–790.

[8]Lang, W., Poinsot, T., and Candel, S, "Active Control of Combustion Instability," *Combustion and Flame*, Vol. 70, No. 3, 1987, pp. 281–289.

[9]Poinsot, T., Bourienne, F., Candel, S., Esposito, E., and Lang, W., "Suppression of Combustion Instabilities by Active Control," *Journal of Propulsion and Power*, Vol. 5 No. 1, 1987, pp. 1363–1370.

[10]Poinsot, T., Veynante, D., Bourienne, F., Candel, S., Esposito, E., and Surget, J., "Initiation and Suppression of Combustion Instabilities by Active Control," *Proceedings of the 22nd Symposium (International) on Combustion*, The Combustion Inst., Pittsburgh, PA, 1988, p. 1363.

[11]Langhorne, P. J., Dowling, A. P., and Hooper, N., "Practical Active Control System for Combustion Oscillations," *Journal of Propulsion and Power*, Vol. 6, No. 3, 1990, p. 324.

[12]Billoud, G., Galland, M. A., Huynh Huu, C., and Candel, S., "Adaptive Active Control of Combustion Instabilities," Combustion Science and Technology, Vol. 81, Nos. 4–6, 1992, pp. 257–283.

[13]Gutmark, E., Parr, T. P., Hanson-Parr, D. M., and Schadow, K. C., "Stabilization of Combustion by Controlling the Turbulent Shear Flow Structure," 7th Symposium on Turbulent Shear Flows, Stanford Univ., Stanford, CA, Aug. 1989.

[14]Gutmark, E., Wilson, K. J., Parr, T. P., and Schadow, K. C., "Feedback Control of MultiMode Combustion Instability," AIAA Paper 92-0778, 1992.

[15]Gulati, A., and Mani, R., "Active Control of Unsteady Combustion-Induced Oscillations," AIAA Paper 90-0270, 1990.

[16]Raghu, S., and Sreenivasan, K. R., "Control of Acoustically Coupled Combustion and Fluid Dynamic Instabilities," AIAA Paper 87-2690, 1987.

[17]Rayleigh, L., *The Theory of Sound*, Dover, New York, 1945.

[18]Neumeier, Y., and Zinn, B. T., "Active Control of Combustion Instabilities with Real Time Observation of Unstable Combustor Modes," AIAA Paper 96-0758, 1996.

[19]Neumeier, Y., and Zinn, B. T., "Experimental Demonstration of Active Control of Combustion Instabilities Using Real Time Modes Observation and Secondary Fuel Injection," 26th International Symposium on Combustion, Naples, Italy, July 1996.

[20]Gaydon, A. G., *Spectroscopy of Flames*, 2nd ed., Chapman & Hall, London.